

## Spin transition of a two-dimensional hole system in the fractional quantum Hall effect

K. Muraki and Y. Hirayama

*NTT Basic Research Laboratories, 3-1 Morinosato-Wakamiya, Atsugi, Kanagawa 243-0198, Japan*

(Received 8 June 1998; revised manuscript received 5 October 1998)

The effect of the complex valence-band Landau-level (LL) structure on the fractional quantum Hall (FQH) effect of a two-dimensional hole system has been studied in a modulation-doped quantum well (QW) with front and back gates. Owing to the spin-orbit interaction and the band mixing in the valence band, changing the potential asymmetry of the QW with the front and back gates allows us to vary the LL structure for a fixed hole density. We observed a remarkable transition in the  $\nu = \frac{4}{3}$  FQH effect with a striking resemblance to the spin transitions observed for tilted-field experiments. Self-consistent effective-mass calculations were carried out to confirm that the transition is driven by the change in the effective Zeeman energy. [S0163-1829(99)51004-7]

The spin configuration of a two-dimensional (2D) electron system (ES) in the fractional quantum Hall (FQH) effect has been an issue of considerable interest.<sup>1-4</sup> It has been shown theoretically that, depending on the Landau-level (LL) filling factor  $\nu$ , many of the FQH states can have a spin-unpolarized or only partially polarized ground state when the Zeeman splitting of the system is sufficiently small.<sup>4</sup> For such  $\nu$ , the spin configuration of the ground state is determined by the interplay between the Coulomb interaction energy  $E_C$ , which depends on the total spin  $S$ , and the Zeeman energy  $E_Z = g\mu_B B S_z$  ( $S_z$ :  $z$  component of  $S$ ).<sup>5</sup> A notable exception is  $\nu = 1/q$  ( $q$ : odd integer), for which the system is ferromagnetic and the ground state is always spin polarized even in the absence of Zeeman energy. Experiments have indeed shown that the FQH states at  $\nu = \frac{3}{5}, \frac{2}{3}, \frac{4}{3}, \frac{7}{5},$  and  $\frac{8}{5}$  undergo a transition between states with different degrees of spin polarization.<sup>1-3</sup> Experimentally, the transitions can be driven either by tilting the sample with respect to the magnetic field or by changing the carrier density. In the former, it is assumed that  $E_C$  depends only on the perpendicular component of  $B$ , while  $E_Z$  is determined by *total*  $B$ . The latter changes the relative size of  $E_Z$  and  $E_C$  on the ground that  $E_Z$  changes linearly with  $B$  while  $E_C$  scales as  $e^2/\epsilon l_0 \propto B^{1/2}$ , where  $l_0$  is the magnetic length and  $\epsilon$  is the background dielectric constant.

Similar angle- (Ref. 6) or density-dependent<sup>7</sup> studies carried out on 2D hole systems (HS's) in GaAs/Al<sub>x</sub>Ga<sub>1-x</sub>As single heterojunctions (SH's) also reported the spin transition of the  $\nu = \frac{4}{3}$  state. The reported data were very similar to those on the ES; the only difference was that the transition occurred at a lower magnetic field in the HS than in the ES. It is, however, rather surprising that the HS behaves so similarly to the ES, for spin is not a good quantum number in HS's as a result of the spin-orbit interaction and the heavy-hole light-hole mixing.<sup>8</sup> In addition, LL mixing is thought to be substantial in HS's, for the heavier hole mass,  $m_h^* \approx 0.38m_e$  ( $m_e$ : free electron mass), reduces the LL separation typically by a factor of 5 compared to that of ES's. Although LL mixing has been shown to reduce the FQH energy gap in HS's,<sup>9</sup> phenomena *qualitatively* different from their counterparts in ES's have not been reported so far. In this paper, we study the FQH effect of a high-mobility 2D

HS in a modulation-doped quantum well (QW) with front and back gates. We demonstrate that a similar spin transition can be driven in a HS by changing the potential asymmetry of the QW and thereby changing the valence-band LL structure, a direct consequence of the spin-orbit interaction and the band mixing in the HS.

The samples used in this study were 20-nm-thick GaAs/Al<sub>0.33</sub>Ga<sub>0.67</sub>As modulation-doped QW structures, which were grown by molecular-beam epitaxy (MBE) on  $n$ -type GaAs (311)A substrates. We investigated two structures with different doping schemes. Sample I is a symmetrically doped QW with 100-nm undoped spacer layers and Si-doped layers on both sides. Sample II is a one-side-doped QW with a 50-nm spacer. Both samples had a low-temperature mobility of about 60 m<sup>2</sup>/Vs for a hole density  $p = 1.8 \times 10^{15} \text{ m}^{-2}$ . These samples were processed into Hall-bar structures (200–400  $\mu\text{m}$  wide) with Au/AuZn Ohmic contacts and a Au front gate. The  $n$ -type substrate served as a back gate,<sup>10</sup> which in conjunction with the front gate allows for the independent control of the hole density and the potential asymmetry of the QW.<sup>11</sup> Magnetotransport measurements were carried out at  $T \approx 50$  mK in a dilution refrigerator. A standard low-frequency ac lock-in technique was employed with a constant current of 20 nA.

Figure 1 shows the evolution of the FQH states observed when the potential asymmetry of the QW was varied for a fixed hole density in sample I. The front-gate bias,  $V_{fg}$ , was varied from (a)  $-0.05$  to (f)  $-0.20$  V. For each  $V_{fg}$ , the back-gate bias was adjusted to keep the hole density constant at  $(1.76 \pm 0.02) \times 10^{15} \text{ m}^{-2}$ . Analyzing the low-field Shubnikov-de Haas oscillations tells us that the QW potential becomes nearly symmetric for  $V_{fg} = -0.05$  V.<sup>11</sup> As a measure of the potential asymmetry, the difference in the hole densities supplied from the front and back sides of the QW,  $\delta p \equiv p_f - p_b$ ,<sup>12</sup> is shown for each trace along with the calculated potential profile and the charge distribution of holes.

For the symmetric potential ( $\delta p = 0.0$ ), well-developed FQH features are observed at  $\nu = \frac{5}{3}$  and  $\frac{4}{3}$  both in the diagonal ( $\rho_{xx}$ ) and Hall ( $\rho_{xy}$ ) resistivities. Higher-order structures, such as  $\nu = \frac{8}{5}$  and  $\frac{7}{5}$ , are not resolved here. As the QW po-

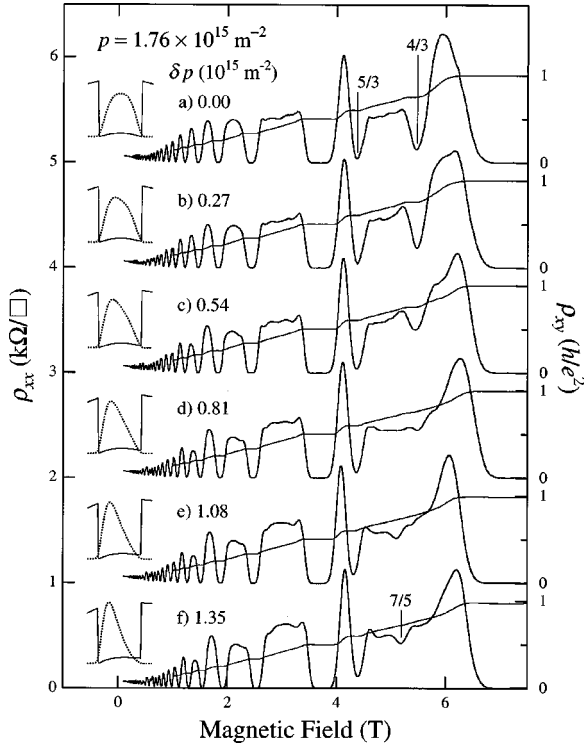


FIG. 1. Effect of potential asymmetry on the FQH effect of sample I. Each  $\rho_{xx}$  trace is offset by  $1 \text{ k}\Omega/\square$ . The calculated potential profile (solid line) and the charge distribution of holes (dotted line) are shown next to each trace.

tential is made progressively asymmetric, the  $\nu = \frac{4}{3}$  state gets weaker and, in turn, a weak feature appears in  $\rho_{xx}$  at  $\nu = \frac{7}{5}$ . Eventually, the  $\nu = \frac{4}{3}$  state completely disappears and the  $\nu = \frac{7}{5}$  state develops as a distinct  $\rho_{xx}$  minimum for  $\delta p = 1.35 \times 10^{15} \text{ m}^{-2}$ . Meanwhile, the strength of the  $\nu = \frac{5}{3}$  state does not change significantly, in contrast to  $\nu = \frac{4}{3}$  and  $\frac{7}{5}$ .

Apparently, these results bear a striking resemblance to the spin transitions reported for ES's (Refs. 1 and 3) and HS's.<sup>6,7</sup> Indeed, we found that similar transitions took place when the sample was tilted with respect to the magnetic field. In Figs. 2(a)–2(c), we compare the data taken at different tilt angles  $\theta$ . For these data, the hole density was fixed at  $1.76 \times 10^{15} \text{ m}^{-2}$  and the QW potential was kept symmetric. Since  $\nu$  is determined by the perpendicular field  $B_{\perp} = B \cos \theta$ , tilting the sample shifts a given  $\nu$  (corresponding to a particular  $B_{\perp}$ ) to a higher field  $B = B_{\perp} / \cos \theta$ , which then increases the Zeeman splitting  $\Delta_Z = |g| \mu_B B$  for the same  $\nu$ . It is seen that the  $\nu = \frac{4}{3}$  state, which appears as a pronounced feature at  $\theta = 0^\circ$ , is almost completely destroyed at  $\theta = 45^\circ$ . Since the increased  $\Delta_Z$  destabilizes the spin-reversed states and does not affect the fully polarized state, this tells us that the  $\frac{4}{3}$  state in the symmetric QW at  $\theta = 0^\circ$  is either unpolarized, or only partially polarized. By a similar argument, it can be said that the  $\frac{4}{3}$  state reemerging at a larger tilt angle  $\theta = 54^\circ$  has a larger degree of polarization. Although the possibility of the partially polarized  $\frac{4}{3}$  state was first discussed in ES's,<sup>1</sup> more recent work by Du *et al.*<sup>3</sup> shows the  $\frac{4}{3}$  states at small and large tilt angles to be unpolarized and fully polarized, respectively. Here, we follow their assignments, and identify in our HS the  $\nu = \frac{4}{3}$  states at  $\theta = 0^\circ$  and  $54^\circ$  as the unpolarized ( $\uparrow\downarrow$ ) and polarized ( $\uparrow\uparrow$ ) states, re-

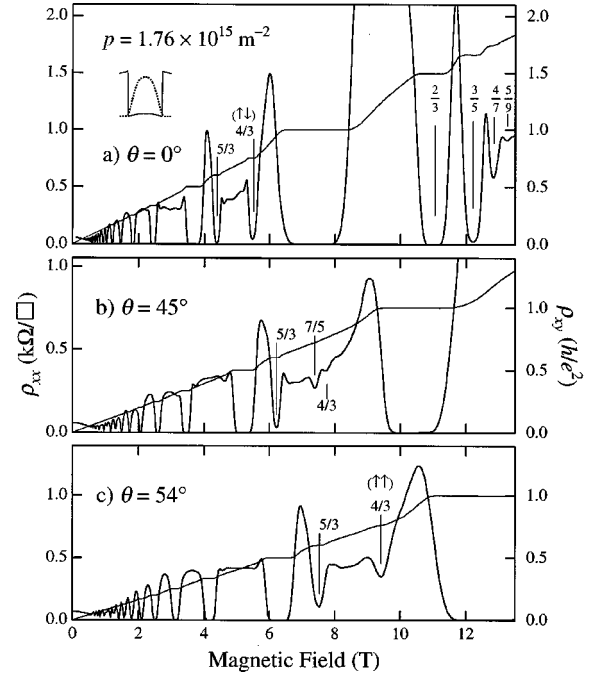


FIG. 2. Magnetotransport data of sample I taken at different tilt angles  $\theta$ . The QW potential is kept symmetric.

spectively. These are also consistent with their density dependence (not shown); the  $\frac{4}{3}$  state at  $\theta = 0^\circ$  ( $54^\circ$ ) persisted for much lower (higher)  $p$ .

Since the spin and the orbital motion are not separable in HS's, the evolution of  $\Delta_Z$  with  $\theta$ , in general, cannot be described in terms of a well-defined  $g$  factor. Indeed, strongly nonlinear behavior of the energy gap at integer  $\nu$  has been observed at very large tilt angles.<sup>13</sup> Nevertheless, the evolution of the integer gap for relatively small  $\theta$  is reported to be almost linear with total  $B$ ,<sup>13</sup> from which one can deduce the effective  $g$  factor.<sup>14</sup> If we simply assume that  $\Delta_Z$  grows in proportion to the total field, we can roughly estimate that  $\Delta_Z$  needs to be enhanced by a factor of 1.4 ( $\sim 1/\cos 45^\circ$ ) and 1.7 ( $\sim 1/\cos 54^\circ$ ), respectively, to destroy and recover the  $\nu = \frac{4}{3}$  state. Employing the effective  $g$  factor,  $g = 1.1$ , deduced for a 20-nm symmetric QW similar to ours<sup>13</sup> allows us to roughly evaluate the corresponding increase in  $\Delta_Z$  to be 0.15 and 0.25 meV.

The behavior of the  $\nu = \frac{7}{5}$  state seen in Figs. 1 and 2 is similar to the previous reports,<sup>1,6</sup> which have been explained in terms of the initial increase in the energy gap and the following collapse of the gap due to the transition to a higher-spin state, both driven by the increase in  $\Delta_Z$ .<sup>3</sup> On the other hand, the consistent stability of the  $\nu = \frac{5}{3}$  state can be understood by the particle-hole symmetry with the spin degree of freedom,  $\nu \leftrightarrow 2 - \nu$ . According to this relation,  $\nu = \frac{5}{3}$  can be regarded as the particle-hole analog of  $\nu = \frac{1}{3}$ , for which the ground state is always spin polarized.<sup>4</sup>

Now we discuss the mechanism behind the spin transition in the asymmetry-dependent experiments. As seen in Fig. 1, when the QW is made more asymmetric, the spatial extent of the hole wave function is reduced and the HS approaches the ideal 2D system. This strengthens the Coulomb interaction,<sup>15</sup> however, one should note that the calculations, which were carried out for the ideal 2D system, show that  $E_C$  at  $\nu = \frac{4}{3}$  is

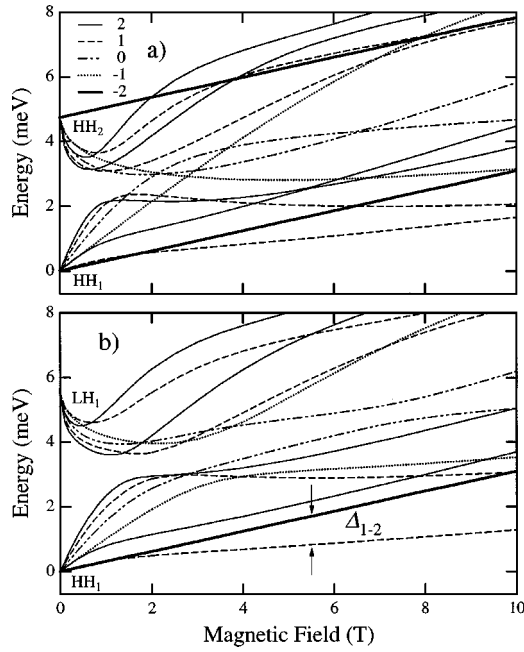


FIG. 3. Valence-band LL structures calculated for a 20-nm QW with (a) symmetric ( $\delta p = 0.0$ ) and (b) asymmetric ( $\delta p = 1.4 \times 10^{15} \text{ m}^{-2}$ ) potentials ( $p = 1.8 \times 10^{15} \text{ m}^{-2}$ ). For clarity, only those LL's emanating from the first and second subbands are shown for  $n$  up to 2. The energy origin is set at the  $\text{HH}_1$  subband edge. [ $\text{HH}_m$  ( $\text{LH}_m$ ) represents the  $m$ th heavy-hole (light-hole) subband.]

minimized for the unpolarized ( $S=0$ ) spin configuration.<sup>4</sup> This is also in line with the experimental observations that the ground state at  $\nu = \frac{4}{3}$  is unpolarized for a small Zeeman splitting.<sup>1,3</sup> Hence, the enhancement of the Coulomb interaction due to squeezing the wave function cannot account for the collapse of the unpolarized  $\frac{4}{3}$  state. Disorder effect, which can arise from the increased probability distribution at the heterointerface and in the barrier alloy, is thought not to be operative here; both zero-field mobility (59 and 57  $\text{m}^2/\text{Vs}$  for the symmetric and the most asymmetric potentials) and  $\rho_{xx}$  at high fields are seen to be almost unchanged.

As described below, our self-consistent effective-mass calculations show that the transition is driven by the increase in the effective Zeeman splitting associated with the change in the QW potential. We first calculated the potential profile by solving the Poisson and Schrödinger equations self-consistently at  $B=0$  using a constant hole mass,  $m_h^* = 0.38m_e$ . The multicomponent effective-mass equation was then solved for each  $B$  using a  $4 \times 4$  Luttinger Hamiltonian with the axial approximation.<sup>16</sup> The Luttinger parameters used are the same as those in Ref. 8. Figure 3 shows the LL structures calculated for the (a) symmetric ( $\delta p = 0$ ) and (b) asymmetric ( $\delta p = 1.4 \times 10^{15} \text{ m}^{-2}$ ) potentials. The calculations reveal that the potential asymmetry of the QW strongly influences the LL structure.

Within a simple picture neglecting LL mixing, the holes occupy only the first and second LL's at  $\nu = \frac{4}{3}$ . We focus our attention to these two LL's that mainly comprise the many-body FQH state. With the axial approximation, which neglects the anisotropy of the valence band in the 2D plane, the envelope functions describing the in-plane motion can be expressed as a set of harmonic-oscillator functions

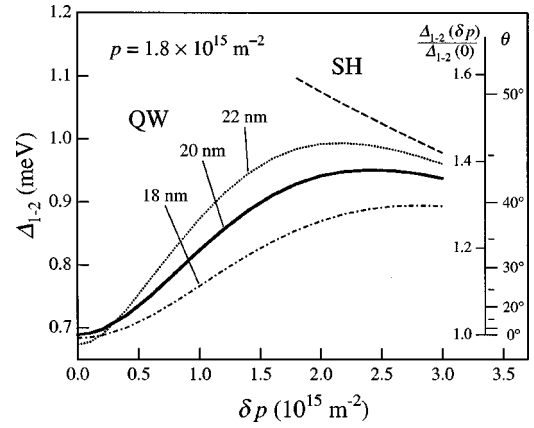


FIG. 4.  $\Delta_{1-2}$  vs  $\delta p$  calculated for QW's with different well widths and a single heterojunction. In the figure, the scale normalized by  $\Delta_{1-2}$  at  $\delta p = 0$  (20-nm QW) is shown to be compared with the tilt angle  $\theta$  for which  $1/\cos \theta$  gives the same value.

$\{\phi_{n+2}, \phi_{n+1}, \phi_n, \phi_{n-1}\}$  ( $n = -2, -1, 0, 1, \dots$ ) for the basis  $\{m_j\} = \{-\frac{3}{2}, -\frac{1}{2}, \frac{1}{2}, \frac{3}{2}\}$ .<sup>8</sup> In Fig. 3, various kinds of lines are used to indicate the value of  $n$  for each LL. It is seen that the first and second LL's have  $n = 1$  and  $-2$ , respectively, in the magnetic field region of interest,  $B \sim 5.5 \text{ T}$  ( $= B_{4/3}$ ). The second LL, having  $n = -2$ , is known to be a pure  $m_j = -\frac{3}{2}$  state.<sup>17</sup> The first LL with  $n = 1$ , on the other hand, is found to be a mixed state dominantly in  $m_j = \frac{3}{2}$ . While the effect of the band mixing on the FQH energy gap has been discussed theoretically,<sup>18</sup> we note that the relative weight of the four  $m_j$ 's in the first LL does not change significantly with the QW potential,<sup>19</sup> which rules out such a band-mixing effect as the origin of the observed transition.

It is important to note that the dominant components of the first and second LL's are  $m_j = \frac{3}{2}$  and  $-\frac{3}{2}$ , respectively, and both of them have  $\phi_0$  harmonic-oscillator envelope function in the 2D plane and ground-subbandlike distribution in the perpendicular direction. Hence, these two LL's can be regarded as the spin-up and spin-down levels of a spin system and their energy separation,  $\Delta_{1-2}$ , as the effective Zeeman splitting. Figure 4 depicts the variation of  $\Delta_{1-2}$  at  $B = 5.5 \text{ T}$  as a function of  $\delta p$ . As  $\delta p$  is varied from 0 to  $1.4 \times 10^{15} \text{ m}^{-2}$ ,  $\Delta_{1-2}$  is seen to increase from 0.69 to 0.88 meV, by a factor of 1.3, in a 20-nm QW. Interestingly, this value, 1.3, is compatible with the angle required to destroy the  $\frac{4}{3}$  ( $\uparrow\downarrow$ ) state in the tilted-field experiments ( $1.4 \sim 1/\cos 45^\circ$ ). Also, the calculated increase in  $\Delta_{1-2}$ , 0.19 ( $= 0.88 - 0.69$ ) meV, is in rough agreement with the value, 0.15 meV, expected from  $g = 1.1$ . These observations confirm that changing the QW potential gives rise to a substantial change in the LL structure that can affect the spin configuration of the FQH state.

As seen in Fig. 4,  $\Delta_{1-2}$  initially increases with  $\delta p$ , but further increasing  $\delta p$  causes  $\Delta_{1-2}$  to first level off and then eventually decline. Indeed, we could not observe the  $\nu = \frac{4}{3}$  ( $\uparrow\uparrow$ ) state even when  $\delta p$  was further increased using the one-side-doped QW (sample II). Figure 5 shows the data obtained from sample II.<sup>20</sup> Similar behavior is observed; the  $\frac{4}{3}$  ( $\uparrow\downarrow$ ) state gets weaker with increasing  $\delta p$ , and disappears for  $\delta p = 2.2 \times 10^{15} \text{ m}^{-2}$ . It is seen, however, that even for  $\delta p$  as large as  $2.8 \times 10^{15} \text{ m}^{-2}$ , the  $\frac{4}{3}$  ( $\uparrow\uparrow$ ) state is yet to develop.<sup>21</sup> One may notice that larger  $\delta p$  is required to de-

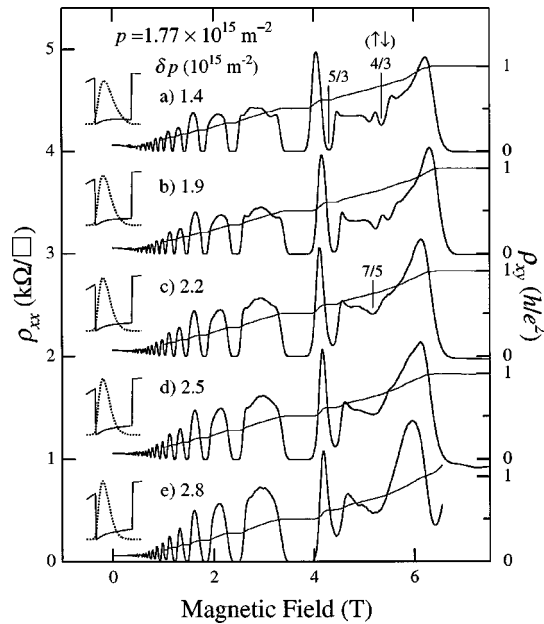


FIG. 5. Effect of potential asymmetry on the FQH effect of sample II. Each  $\rho_{xx}$  trace is offset by 1 k $\Omega/\square$ . The calculated potential profile (solid line) and the charge distribution of holes (dotted line) are shown next to each trace.

stroy the  $\frac{4}{3}$  ( $\uparrow\downarrow$ ) state in sample II than in sample I. This can be understood as due to unintentional difference in the well width that can arise from the drift and/or spatial nonuniformity of the Ga beam flux. By assuming a smaller well width of 18 nm for sample II, the two sets of data can be explained in a coherent manner (see Fig. 4). It is also interesting to note

in Fig. 5 that the  $\rho_{xx}$  minima at  $\nu = \frac{7}{5}$  gets broader with increasing  $\delta p$ , and becomes no more discernible for  $\delta p \geq 2.5 \times 10^{15} \text{ m}^{-2}$ , suggestive of the spin transition of the  $\frac{7}{5}$  state. Indeed, noticeable resemblance is found between the traces (c)–(e) and the angle-dependent data in Ref. 6. This, however, must be examined carefully with further investigation, for the disorder effect is apparent for the largest  $\delta p$ , where  $\nu = \frac{5}{3}$  is seen to weaken.

Finally, we briefly mention that the dependence of  $\Delta_{1-2}$  on the confinement potential discussed here can account for some aspects of the previously reported data. Rodgers *et al.*<sup>7</sup> reported in their density-dependent study that the  $\frac{4}{3}$  ( $\uparrow\uparrow$ ) state already appeared for  $p \geq 1.4 \times 10^{15} \text{ m}^{-2}$  in their SH sample, while in our QW samples the  $\frac{4}{3}$  ( $\uparrow\uparrow$ ) state did not emerge for  $p$  up to  $1.8 \times 10^{15} \text{ m}^{-2}$ . As seen in Fig. 4,  $\Delta_{1-2}$  becomes considerably larger in SH's than in QW's. For the ideal case of no depletion charge ( $\delta p = p$ ),<sup>22</sup>  $\Delta_{1-2}$  becomes 1.6 times that of a symmetric QW, large enough for the  $\frac{4}{3}$  ( $\uparrow\uparrow$ ) state to develop. Also, the largely sample-dependent behavior of the SH's in Ref. 6 can be ascribed, in part, to the dependence of  $\Delta_{1-2}$  on the depletion charge,<sup>22</sup> which makes  $\Delta_{1-2}$  somewhat sample-dependent in SH's.

In summary, we have studied the effect of the confinement potential on the FQH effect of a 2D HS. We have demonstrated that changing the confinement potential strongly modifies the valence-band LL structure via the spin-orbit interaction and the band mixing, which can give rise to the spin transition of the  $\nu = \frac{4}{3}$  FQH state.

The authors thank Y. Tokura for his helpful discussions and T. Saku for his technical support with the MBE. The authors are also grateful to Dr. T. Machida and Professor S. Komiyama of The University of Tokyo for their kind cooperation in the initial stage of the work.

- <sup>1</sup>R. G. Clark *et al.*, Phys. Rev. Lett. **62**, 1536 (1989).
- <sup>2</sup>J. P. Eisenstein *et al.*, Phys. Rev. Lett. **62**, 1540 (1989); Phys. Rev. B **41**, 7910 (1990); L. W. Engel *et al.*, *ibid.* **45**, 3418 (1992).
- <sup>3</sup>R. R. Du *et al.*, Phys. Rev. Lett. **75**, 3926 (1995); Phys. Rev. B **55**, R7351 (1997).
- <sup>4</sup>F. C. Zhang and T. Chakraborty, Phys. Rev. B **30**, 7320 (1984); P. A. Maksym, J. Phys.: Condens. Matter **1**, 6299 (1989); T. Chakraborty, Surf. Sci. **229**, 16 (1990).
- <sup>5</sup>Since the lowest  $E_Z$  for each  $S$  is given by  $E_Z = -|g|\mu_B B S$ , the  $E_Z$  term makes larger  $S$  energetically favorable.
- <sup>6</sup>A. G. Davies *et al.*, Phys. Rev. B **44**, 13 128 (1991); Surf. Sci. **263**, 81 (1992).
- <sup>7</sup>P. J. Rodgers *et al.*, J. Phys.: Condens. Matter **5**, L565 (1993).
- <sup>8</sup>U. Ekenberg and M. Altarelli, Phys. Rev. B **32**, 3712 (1985).
- <sup>9</sup>H. C. Manoharan *et al.*, Phys. Rev. Lett. **73**, 3270 (1994).
- <sup>10</sup>M. Y. Simmons *et al.*, Appl. Phys. Lett. **70**, 2750 (1997).
- <sup>11</sup>K. Muraki and Y. Hirayama, Physica B **249–251**, 65 (1998).
- <sup>12</sup> $\delta p$  can be calculated as  $\delta p = 2(\partial p / \partial V_{fg})(V_{fg} - V_{fg}^{\text{sym}})$ , where  $V_{fg}^{\text{sym}}$  is the front-gate bias for the symmetric potential.
- <sup>13</sup>A. J. Daneshvar *et al.*, Phys. Rev. Lett. **79**, 4449 (1997).
- <sup>14</sup>The term ‘‘effective  $g$  factor’’ must be used with care, for it is not a well-defined material constant, and can depend on the well width, carrier density, field direction, etc.
- <sup>15</sup>F. C. Zhang and S. Das Sarma, Phys. Rev. B **33**, 2903 (1986); D. Yoshioka, J. Phys. Soc. Jpn. **55**, 885 (1986).
- <sup>16</sup>For simplicity, the calculations were done for a (001) heterostructure.
- <sup>17</sup>Setting  $n = -2, -1$ , and 0 in  $\{\phi_{n+2}, \phi_{n+1}, \phi_n, \phi_{n-1}\}$  results in negative indices for some of the harmonic-oscillator functions, whose coefficients are then automatically set to zero. Accordingly, those states with  $n = -2$  have only  $m_j = -\frac{3}{2}$ .
- <sup>18</sup>A. H. MacDonald and U. Ekenberg, Phys. Rev. B **39**, 5959 (1989); S.-R. E. Yang, A. H. MacDonald, and D. Yoshioka, *ibid.* **41**, 1290 (1990).
- <sup>19</sup>The relative weight of the four  $m_j$ 's in the first LL at  $B = 5.5$  T was calculated to be  $(f_{-3/2}, f_{-1/2}, f_{1/2}, f_{3/2}) = (0.025, 0.185, 0.024, 0.766)$  and  $(0.028, 0.134, 0.081, 0.757)$  for the symmetric and asymmetric potentials, respectively.
- <sup>20</sup>Here,  $\delta p$  was evaluated by setting  $p_f = 1.3 \times 10^{15} \text{ m}^{-2}$  for  $V_{fg} = 0$  V, as expected from the 50-nm spacer thickness.
- <sup>21</sup>For the largest  $\delta p$ , peculiar behavior occurs at  $B \geq 6.4$  T, probably because the low-density hole gas in the ‘‘lead’’ regions, being depleted by the large back-gate bias, becomes highly resistive at large fields.
- <sup>22</sup>Since the depletion charge  $N_d (\geq 0)$  decreases the holes as  $p = p_f - N_d$  in SH's,  $\delta p$  is given by  $\delta p = p + 2N_d (\geq p)$ .